WATER RESOURCES RESEARCH, VOL. 36, NO. 12, PAGES 3467–3479, DECEMBER 2000

On the late-time behavior of tracer test breakthrough curves

Roy Haggerty
Department of Geosciences, Oregon State University, Corvallis

Sean A. McKenna and Lucy C. Meigs
Geohydrology Department, Sandia National Laboratories, Albuquerque, New Mexico

Abstract. We investigated the late-time (asymptotic) behavior of tracer test breakthrough curves (BTCs) with rate-limited mass transfer (e.g., in dual-porosity or multiporosity systems) and found that the late-time concentration c is given by the simple expression $c = t_{ad}\{c_0 g - [m_0(\partial g/\partial t)]\}$, for $t \gg t_{ad}$ and $t_\alpha \gg t_{ad}$, where t_{ad} is the advection time, c_0 is the initial concentration in the medium, m_0 is the zeroth moment of the injection pulse, and t_α is the mean residence time in the immobile domain (i.e., the characteristic mass transfer time). The function g is proportional to the residence time distribution in the immobile domain; we tabulate g for many geometries, including several distributed (multirate) models of mass transfer. Using this expression, we examine the behavior of late-time concentration for a number of mass transfer models. One key result is that if rate-limited mass transfer causes the BTC to behave as a power law at late time (i.e., $c \sim t^{-k}$), then the underlying density function of rate coefficients must also be a power law with the form α^{k-3} as $\alpha \to 0$. This is true for both density functions of first-order and diffusion rate coefficients. BTCs with $k < 3$ persisting to the end of the experiment indicate a mean residence time longer than the experiment, and possibly an infinite residence time, and also suggest an effective rate coefficient that is either undefined or changes as a function of observation time. We apply our analysis to breakthrough curves from single-well injection-withdrawal tests at the Waste Isolation Pilot Plant, New Mexico.

1. Introduction

Mass transfer continues to be cited as a critical transport process in groundwater, soils, and streams. Estimation of rate coefficients (for both diffusion and sorption) is highly sensitive to the late-time behavior of breakthrough curves (BTCs). Indeed, recent studies have shown that the late-time data (i.e., after the advective peak has passed) may be the most important data for estimation of both the capacity coefficient and the rate coefficient or density function of rate coefficients [e.g., *Farrell and Reinhard*, 1994; *Wagner and Harvey*, 1997; *Werth et al.*, 1997; *Haggerty and Gorelick*, 1998; *Haggerty et al.*, 2001]. With improvements in experimental and analytical techniques, concentration observations are now frequently available from laboratory and field experiments over several orders of magnitude of both time and concentration. Therefore the examination of late-time behavior of BTCs is both feasible and critically important to the evaluation of rate-limited mass transfer, particularly if discrimination between different models of mass transfer is desired.

A rapidly growing body of recent work on mass transfer and transport has extended the basic model of single-rate mass transfer [e.g., *Coats and Smith*, 1964; *van Genuchten and Wierenga*, 1976; *Cameron and Klute*, 1977; *Rao et al.*, 1980] or two-rate mass transfer [e.g., *Brusseau et al.*, 1989] to models with distributed or multiple rates of mass transfer described by a density function of rate coefficients and primarily applied to laboratory data [*Connaughton et al.*, 1993; *Lafolie and Hayot*, 1993; *Pedit and Miller*, 1994, 1995; *Backes et al.*, 1995; *Chen and Wagenet*, 1995; *Haggerty and Gorelick*, 1995; *Ahn et al.*, 1996; *Chen and Wagenet*, 1997; *Culver et al.*, 1997; *Cunningham et al.*, 1997; *Sahoo and Smith*, 1997; *Werth et al.*, 1997; *Cunningham and Roberts*, 1998; *Deitsch et al.*, 1998; *Haggerty and Gorelick*, 1998; *Kauffman et al.*, 1998; *Lorden et al.*, 1998; *McLaren et al.*, 1998; *Hollenbeck et al.*, 1999; *Stager and Perram*, 1999]. It should be noted, however, that the concept of multiple timescales of mass transfer has been employed for at least 3 decades, primarily in chemical engineering and soil physics [*Ruthven and Loughlin*, 1971; *Villermaux*, 1981; *Rao et al.*, 1982; *Neretnieks and Rasmuson*, 1984; *Rasmuson*, 1985; *Fong and Mulkey*, 1990; *Valocchi*, 1990], as have multiple timescales of reaction in chemistry [e.g., *Albery et al.*, 1985].

A power law BTC (i.e., $c \sim t^{-k}$) plots as a straight line on a double-logarithmic graph. Consequently, in this paper we will frequently refer to the value of the power k as the "slope." Although the slope is always negative, for the sake of brevity, we will refer only to its absolute value.

Power law behavior at late time in BTCs has been noted in a number of laboratory and field experiments. Power law behavior was observed in single-well injection-withdrawal (SWIW) tests conducted in a fractured dolomite in New Mexico [*Meigs and Beauheim*, 2001]. After pulse injections of solute the BTC data in five SWIW tests showed power law behavior at late time with k ranging from 2.1 to 2.8. While a lognormal density function of diffusion rate coefficients provided excellent matches to the data [*Haggerty et al.*, 2001], the details of the power law behavior were left for another paper. *Farrell and Reinhard* [1994] and *Werth et al.* [1997] observed power law

Copyright 2000 by the American Geophysical Union.

Paper number 2000WR900214.
0043-1397/00/2000WR900214$09.00

BTC and mass recovery curves with sorbing organic solutes in unsaturated media. *Cunningham et al.* [1997] were able to represent the *Werth et al.* [1997] data with a gamma density function of diffusion rate coefficients, while *Haggerty and Gorelick* [1998] were able to approximate the power law behavior with a lognormal density function of diffusion rate coefficients. Both *Cunningham et al.* [1997] and *Haggerty and Gorelick* [1998] noted the inability of conventional models of mass transfer to yield the appropriate power law behavior. Power law behavior with a slope of 3/2 has been observed in field data from the Grimsel, Switzerland, test site and has been adequately explained with conventional (single rate) matrix diffusion [*Eikenberg et al.*, 1994; *Hadermann and Heer*, 1996]. However, single-rate diffusion is only able to yield a power law of exactly $t^{-3/2}$ and can only maintain this behavior slightly longer than the mean immobile-domain residence time ($t_\alpha = a^2/15D_a$ for spheres and $a^2/3D_a$ for layers), where D_a is the apparent diffusivity and a is the half thickness of the immobile domain. Power law behavior such as that observed by *Farrell and Reinhard* [1994]; *Werth et al.* [1997], or *Meigs and Beauheim* [2001] cannot be explained with conventional single-rate diffusion. *Jaekel et al.* [1996] showed that power law BTCs can result from a pulse injection of solute and equilibrium Freundlich sorption. Unfortunately, none of the three data sets mentioned above are explained by this (the Meigs and Beauheim tracers were nonsorbing, and equilibrium Freundlich sorption is insufficient to explain the power laws in the other data sets [*Werth et al.*, 1997]).

The purpose of this paper is to explore the nature of tailing in mobile-immobile (dual porosity) tracer test BTCs for a wide variety of linear mass transfer models. Specifically, we have the following objectives: (1) develop an analytic expression for the late-time BTCs for transport experiencing a distribution of either first-order sorption or diffusion timescales and for both pulse injections and media with nonzero initial concentrations, (2) examine the information that can be provided by the late-time behavior of the BTC, and (3) examine BTCs that exhibit power law behavior at late time and the implications for mass transfer. Particular expressions describing the late-time BTCs for single-rate models with both infinite and finite immobile domains, as well as multirate models with first-order and diffusion rate coefficients defined by lognormal, gamma, and power law density functions, are provided. Implications of the late-time slopes defined by these equations are discussed with respect to mass transfer processes, including implications for estimates of the mean residence time in the immobile domain (or, equivalently, a characteristic mass transfer time). The power law late-time behavior of BTCs in two SWIW tests from the Waste Isolation Pilot Plant (WIPP) site in New Mexico are examined.

2. Mathematical Development

2.1. General Case: Late-Time Solution for Concentration

The mass balance equation for a solute advecting and dispersing in one dimension (i.e., along a single stream tube) and interacting with rock via diffusion, linear equilibrium sorption, and/or linear nonequilibrium sorption is

$$\frac{1}{R_a}\frac{\partial}{\partial x}\left(\alpha_L v \frac{\partial c}{\partial x} - vc\right) = \frac{\partial c}{\partial t} + \Gamma(x, t), \tag{1}$$

where c [$M\ L^{-3}$] is solute concentration, α_L [L] is longitudinal dispersivity, v [$L\ T^{-1}$] is pore fluid velocity, R_a [dimensionless] is the retardation factor in the mobile (advective, effective, or kinematic) porosity, c [$M\ L^{-3}$] is solute concentration within the advective porosity, and $\Gamma(x, t)$ [$M\ L^{-3}\ T^{-1}$] is the source-sink term for mass exchange with the immobile (matrix or diffusive) porosity and nonequilibrium sorption sites. From this point forward, we will adopt the terminology of "mobile" and "immobile" domains and concentrations, which refer to either sorption or diffusion. We will employ the uniform initial conditions

$$c(x, t = 0) = c_{im}(x, z, t = 0) = c_0, \tag{2a}$$

where c_{im} [$M\ L^{-3}$] is solute concentration within the immobile domain, which may, in the case of diffusion, be a function of a second spatial coordinate z oriented normal to the mobile-immobile domain interface. We will also employ the boundary conditions

$$c(x = 0, t) = m_0\delta(t), \tag{2b}$$

$$c(x \to \infty, t) = c_0, \tag{2c}$$

where m_0 [$M\ T\ L^{-3}$] is the zeroth moment of the BTC, c_0 [$M\ L^{-3}$] is the initial concentration in the system, and $\delta(t)$ [T^{-1}] is the Dirac delta. The Dirac injection is never met in practice. However, as long as the duration of the pulse is much shorter than the mean residence time in the immobile domain, (2b) will be a sufficiently good approximation. For a finite pulse injection with constant velocity the zeroth moment m_0 is the injected concentration multiplied by injection time.

For initial and boundary conditions (2a)–(2c) then at late time,

$$\alpha_L \frac{\partial c}{\partial x} \ll c, \qquad t \gg t_{ad}, \tag{3}$$

where t_{ad} [T] is the average advective residence time (equal to LR_a/v if velocity and retardation are constant in space). In other words, once the input pulse has advected far past the point of observation L, then dispersion has a negligible effect on concentration. Figure 1 (discussed in section 3.2) shows that the late-time result we obtain is valid independent of the dispersivity. Note that (3) is always valid (including early time) if $\alpha_L \ll L$. Similarly, if the immobile domain has a long mean residence time relative to advection, then at late time

$$\frac{\partial c}{\partial t} \ll \Gamma(x, t), \qquad t \gg t_{ad} \qquad t_\alpha \gg t_{ad}, \tag{4}$$

where t_α [T] is the mean residence time in the immobile domain. At late time, concentrations do not change significantly with time, and changes of concentration along the streamline are determined by exchange between the mobile and immobile domains. In other words, at late time, concentration at any point in space is determined only by the sum of diffusion out of the immobile domain between the point of injection and the point of interest. Note that from this point forward, it will be assumed that $t_\alpha \gg t_{ad}$ and $t \gg t_{ad}$ unless otherwise stated. Therefore (1) may be rewritten:

$$-\frac{v}{R_a}\frac{\partial c}{\partial x} = \Gamma(x, t), \tag{5}$$

where we have assumed that there are no sources and sinks of fluid and velocities are steady (note, however, that v and R_a

may still be variable in space). By integration we can obtain a solution for concentration at late time:

$$c(x = L, t) = -\int_0^L \frac{R_a(x)}{v(x)} \Gamma(x, t)\, dx, \qquad (6)$$

where L [L] is the distance from point of injection to point of observation along the flow path. Note that the integration over space is valid because at late time the source-sink term changes very slowly relative to the advective residence time. If the parameters and functions that compose $\Gamma(x, t)$ are spatially uniform (the spatially variable case is left for a future paper), then this leaves us with a very simple expression for concentration at late time:

$$c(x = L, t) = -t_{ad}\Gamma(t). \qquad (7)$$

Note that this expression is valid even if the velocity field is not spatially uniform. From this point on, the dependency of c on $x = L$ and t is assumed implicitly.

2.2. Source-Sink Term $\Gamma(t)$

The source-sink term $\Gamma(t)$ is the rate of loss or gain of concentration to or from the immobile domain (loss at early time and gain at late time). The source-sink is commonly expressed as a derivative of immobile concentrations [e.g., *van Genuchten and Wierenga*, 1976; *Cameron and Klute*, 1977], but for our problem it is more convenient to express it as a convolution, following *Carrera et al.* [1998]. For any linear mass transfer problem with uniform initial conditions the source-sink term at all times is

$$\Gamma(t) = \int_0^t \frac{\partial c(t-\tau)}{\partial \tau} g(\tau)\, d\tau = \frac{\partial c}{\partial t} * g = c * \frac{\partial g}{\partial t} + c g_0 - c_0 g \qquad (8)$$

where $g(\tau)$ is a "memory function" to be defined [T^{-1}], the asterisk represents the convolution product, g_0 is the memory function at $t = 0$ [T^{-1}], and c_0 [$M\ L^{-3}$] is the initial concentration. Note that the Laplace transform of (8) is commonly used in analytical solutions [e.g., *Villermaux*, 1974; *Carrera et al.*, 1998; *Cunningham and Roberts*, 1998; *Hollenbeck et al.*, 1999] and that the right-hand-side of (8) is most easily derived in the Laplace domain. Equation (8) has been expressed explicitly in the time domain by, for example, *Peszyńska* [1996] and *Carrera et al.* [1998], and results in an integro-partial differential equation when substituted back into (1). The memory function $g(t)$ may be physically interpreted as the capacity coefficient (β_{tot} (see Appendix A)) multiplied by the residence time distribution in the immobile domain, given a Dirac pulse at the surface. The derivative of $g(t)$ is proportional to what is commonly called in statistical physics the probability of first return or distribution of first passage times [e.g., *Bouchaud and Georges*, 1990, pp. 271–272].

We desire to find a closed-form expression for the source-sink term in (8), accurate at late time, that may be substituted into (7). We recognize the following characteristics of $\Gamma(t)$: (1) At early time the function represents rapid loss from a high-concentration pulse in the mobile domain to the immobile domain, and (2) at late time the function represents slow gain to the mobile domain (which has very low concentration) from the immobile domain. To obtain a solution that is accurate at late time, we therefore require an approximate function for mobile-domain concentration that has the correct pulse size at early time and that is approximately zero at late time. Such an approximation is available in $c \cong m_0\delta(t)$, where m_0 is the zeroth moment of the injection. Note that this approximation is used only for calculating the source-sink term and not as an approximation for late-time concentration itself. This approximation works because at late time the source-sink term does not strongly retain "memory" of the details of the input but only of the magnitude of the input. That this approximation is sufficient will become apparent when the results are compared to full numerical solution. Employing the properties of convolution, (8) can now be expressed:

$$\Gamma(t) \cong m_0 \frac{\partial g}{\partial t} - c_0 g, \qquad t \gg t_{ad} \qquad t_\alpha \gg t_{ad}. \qquad (9)$$

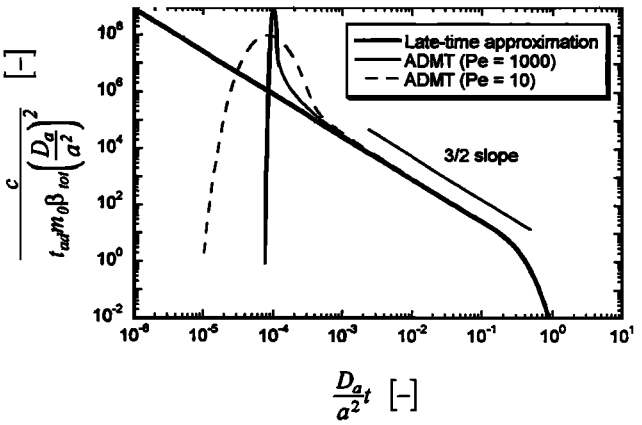

Figure 1. Late-time solution and full advection-dispersion mass transfer (ADMT) solutions (Pe = 10 and 1000) for spherical diffusion.

The general form of the memory function is (modified from *Carrera et al.* [1998, p. 182])

$$g(t) = \int_0^\infty \alpha b(\alpha) e^{-\alpha t}\, d\alpha, \qquad (10)$$

where α is a rate coefficient [T^{-1}] and $b(\alpha)$ is a density function of first-order rate coefficients [T]. Note two differences between our definition of the memory function and that of *Carrera et al.* [1998, p. 182, Equations (15) and (16)]. First, our memory function $g(t)$ includes the constants that are placed before the source-sink term in Carrera et al.'s mass balance equation. Second, although *Carrera et al.* [1998] express (10) as a discrete function, the more general expression is as a continuous function, allowing for density functions of diffusion rate coefficients, etc. Various density functions $b(\alpha)$ are given in Table 1 along with the corresponding memory function $g(t)$. Note that using (15) from *Carrera et al.* [1998, p. 182] is equivalent to using our (10) for diffusion in a finite layer (see Table 1).

We note that (10) is the Laplace transform of $\alpha b(\alpha)$, where t substitutes for the Laplace variable. We also use the property of the Laplace transform [e.g., *Roberts and Kaufman*, 1966, p. 4]

$$\mathcal{L}\{\alpha^2 b(\alpha)\} = -\frac{\partial g}{\partial t}, \qquad (11)$$

where $\mathcal{L}\{\ \}$ indicates the Laplace transform.

Table 1. Density Functions $b(\alpha)$, Corresponding Memory Functions $g(t)$, and Harmonic Means $\hat{\alpha}_H$ of the Density Functions

Model	$b(\alpha)$	$g(t)$	$\hat{\alpha}_H$
First order	$\beta_{tot}\delta(\alpha - \alpha_f)$	$\alpha_f\beta_{tot}e^{-\alpha_f t}$	α_f
Multirate	$b(\alpha)$	$\int_0^\infty \alpha b(\alpha)e^{-\alpha t}\,d\alpha$	$\beta_{tot}\left(\int_0^\infty \frac{b(\alpha)}{\alpha}d\alpha\right)^{-1}$
Gamma distribution	$\frac{\beta_{tot}}{\gamma^\eta\Gamma(\eta)}\alpha^{\eta-1}e^{-\alpha/\gamma}$	$\beta_{tot}\gamma\eta(\gamma t + 1)^{-\eta-1}$	0 $\eta \le 1$ $(\eta-1)\gamma$ $\eta > 1$
Power law distribution with $\alpha_{min} = 0$[a]	$\sim\alpha^{k-3}$	$\sim t^{1-k}$	0 $k \le 3$ $\frac{(k-3)}{(k-2)}\alpha_{max}$ $k > 3$
Diffusion: finite layer	$\sum_{j=1}^{\infty}\frac{8\beta_{tot}}{(2j-1)^2\pi^2}\delta\left[\alpha - \frac{(2j-1)^2\pi^2}{4}\frac{D_a}{a^2}\right]$	$\sum_{j=1}^{\infty}2\beta_{tot}\frac{D_a}{a^2}\exp\left[-\frac{(2j-1)^2\pi^2}{4}\frac{D_a}{a^2}t\right]$	$3\frac{D_a}{a^2}$
Diffusion: infinite layer[b]	$\lim_{a\to\infty}\sum_{j=1}^{\infty}\frac{8R_{im}\theta_{im}a_w a}{(2j-1)^2\pi^2 R_a}\delta\left[\alpha - \frac{(2j-1)^2\pi^2}{4}\frac{D_a}{a^2}\right]$	$\frac{\theta_{im}R_{im}a_w}{R_a}\sqrt{\frac{D_a}{\pi t}}$	0
Diffusion: cylinder[c]	$\sum_{j=1}^{\infty}\frac{4\beta_{tot}}{u_j^2}\delta\left[\alpha - u_j^2\frac{D_a}{a^2}\right]$	$\sum_{j=1}^{\infty}4\beta_{tot}\frac{D_a}{a^2}\exp\left[-u_j^2\frac{D_a}{a^2}t\right]$	$8\frac{D_a}{a^2}$
Diffusion: sphere	$\sum_{j=1}^{\infty}\frac{6\beta_{tot}}{j^2\pi^2}\delta\left[\alpha - j^2\pi^2\frac{D_a}{a^2}\right]$	$\sum_{j=1}^{\infty}6\beta_{tot}\frac{D_a}{a^2}\exp\left[-j^2\pi^2\frac{D_a}{a^2}t\right]$	$15\frac{D_a}{a^2}$
Diffusion: lognormal D_a/a^{2}[d]	$\sum_{j=1}^{\infty}\frac{8\beta_{tot}}{\sqrt{2\pi^5}(2j-1)^2\sigma\alpha}\exp\left\{-\left[\frac{\ln\left(\frac{4\alpha}{(2j-1)^2\pi^2}\right)-\mu}{2\sigma^2}\right]^2\right\}$	must be obtained numerically	$3\exp\left(\mu - \frac{\sigma^2}{2}\right)$
Diffusion: Gamma D_a/a^{2}[d]	$\sum_{j=1}^{\infty}\frac{8\beta_{tot}}{(2j-1)^2\pi^2\Gamma(\eta)\alpha}\left[\frac{4\alpha}{\gamma(2j-1)^2\pi^2}\right]^\eta\exp\left[-\frac{4\alpha}{\gamma(2j-1)^2\pi^2}\right]$	$\sum_{n=1}^{\infty}2\beta_{tot}\gamma\eta\left[\gamma t\frac{(2j-1)^2\pi^2}{4}+1\right]^{-\eta-1}$	0 $\eta \le 1$ $3(\eta-1)\gamma$ $\eta > 1$

[a]See text and equations (30)–(37) and Table 2 for other cases and details.
[b]R_{im} [dimensionless] is matrix retardation factor; θ_{im} [dimensionless] is matrix porosity; a_w $[L^{-1}]$ is the specific surface area of matrix.
[c]Here u_j is the jth solution of $J_0(u_j) = 0$, where J_0 is a Bessel function of the first kind.
[d]This is a distribution of one-dimensional pathways or layers.

Employing (7), (9), (10), and (11), we can now write an approximation for concentration at late time:

$$c = t_{ad}\left(c_0 g - m_0\frac{\partial g}{\partial t}\right),$$

$$= t_{ad}\int_0^\infty (c_0 + \alpha m_0)\alpha b(\alpha)e^{-\alpha t}\,d\alpha,$$

$$= t_{ad}\mathcal{L}\{(c_0 + \alpha m_0)\alpha b(\alpha)\}. \quad (12)$$

Equation (12) was verified against a numerical model. The numerical model solved the full advection-dispersion mass transfer (ADMT) equations (i.e., (1)) for several types of source-sink terms, Γ. These numerical solutions are discussed in section 3 and shown for several cases in Figures 1–4. The numerical solution required none of the assumptions required to develop (12).

All forms of (12) are equivalent and are useful in different ways for understanding the late-time behavior of BTCs. We expect that in most applications only one of c_0 or m_0 will be nonzero; however, (12) holds true regardless of the values of the initial concentration in the porous medium c_0 and the zeroth temporal moment of the input pulse m_0. Note that the late-time concentration can be calculated for various density functions $b(\alpha)$ using $g(t)$ supplied in Table 1. See Appendix B for two notes regarding the use of (12).

At this point we reemphasize the restrictions on (12). These are as follows: (1) Time is much greater than the advection time; (2) the mean residence time in the immobile domain is much greater than the advection time; and (3) time is much greater than the duration of the injection pulse, meaning that an impulse (Dirac) function is a valid approximation to the injection. In a spatially varying velocity field, restrictions (1) and (2) mean that both time and mean residence time in the immobile domain must be much greater than the sum of advection time across a control plane and the standard deviation of that advection time. In particular, a power law distribution of advection times (such as invoked by, for example, *Berkowitz and Scher* [1997]) would invalidate the use of (12).

2.3. Mean Residence Time in Immobile Domain

One of the criteria for use of (12) is that the mean residence time in the immobile domain be much greater than the advection time. This section outlines the calculation of this mean residence time, as well as providing an effective rate coefficient that may be used in an "equivalent" first-order model of mass transfer.

The residence time distribution in the immobile domain given a Dirac impulse at the surface is $g(t)/\beta_{tot}$. The mean

residence time (or characteristic mass transfer time) is therefore

$$t_\alpha = \frac{1}{\beta_{tot}} \int_0^\infty t g(t)\, dt = \frac{1}{\beta_{tot}} \int_0^\infty \frac{b(\alpha)}{\alpha}\, d\alpha. \quad (13)$$

It can be shown [e.g., *Cunningham and Roberts*, 1998] that the zeroth, first, and second temporal moments of the BTC are the same for any density function of rate coefficients provided that the mean residence time in the immobile domain is the same. Therefore the best effective rate coefficient (i.e., the one that yields the same zeroth, first, and second moments of the BTC) is the harmonic mean of the density function, since

$$\hat{\alpha}_H = \frac{1}{t_\alpha} = \beta_{tot}\left(\int_0^\infty \frac{b(\alpha)}{\alpha}\, d\alpha \right)^{-1}. \quad (14)$$

Notably, the harmonic mean may be zero for some density functions, meaning that the mean residence time in the immobile domain is infinite. Note that an infinite mean residence time does not require infinite size or infinite capacity in the immobile domain. The harmonic means for a number of density functions $b(\alpha)$ are shown in Table 1.

3. Late-Time Behavior of BTCs

In this section we will consider a number of examples of BTCs after a pulse injection into a medium with zero initial concentration. Many of the functions developed in this section are summarized in Table 1, as are several others not discussed here.

3.1. Simple Example 1: First-Order Mass Transfer

Consider the simplest case of mass transfer described by a single first-order rate coefficient α_f. The density function of rate coefficients is

$$b(\alpha) = \beta_{tot}\delta(\alpha - \alpha_f). \quad (15)$$

The memory function $g(t)$, given by applying (10) to (15), is

$$g(t) = \alpha_f \beta_{tot} e^{-\alpha_f t}. \quad (16)$$

The resulting late-time approximation for concentration in the mobile domain (with initial concentration of zero) is given by substituting (16) into (12):

$$c = m_0 t_{ad} \beta_{tot} \alpha_f^2 e^{-\alpha_f t}. \quad (17)$$

This solution displays the well-known behavior that late-time concentration is exponential with a semilog slope $d(\ln c)/dt$ of $-\alpha_f$.

3.2. Simple Example 2: Finite Spherical Blocks

Consider the case of diffusion into finite spherical matrix blocks. *Haggerty and Gorelick* [1995] showed that a particular discrete density function of first-order rate coefficients results in a model that is mathematically identical, from the perspective of the mobile domain concentrations, to that of diffusion into and out of various matrix geometries. Using mathematics that is similar to that presented in this paper, *Carrera et al.* [1998] make the same assertion. In the case of spherical blocks the density function is

$$b(\alpha) = \sum_{j=1}^{\infty} \frac{6\beta_{tot}}{j^2\pi^2} \delta\left(\alpha - j^2\pi^2 \frac{D_a}{a^2} \right) \quad (18)$$

where β_{tot} [dimensionless] is the capacity coefficient of the spherical blocks, D_a [$L^2\ T^{-1}$] is the apparent diffusivity, and a [L] is the radius of the spherical blocks. This density function is a series of Dirac deltas with monotonically decreasing weight. The harmonic mean of (18) is the well-known linear driving force approximation 15 D_a/a^2 [e.g., *Glueckauf*, 1955], and the mean residence time in the spheres is therefore $t_\alpha = a^2/15D_a$. The memory function is

$$g(t) = \sum_{j=1}^{\infty} 6\beta_{tot} \frac{D_a}{a^2} \exp\left(-j^2\pi^2 \frac{D_a}{a^2} t \right). \quad (19)$$

Readers familiar with diffusion in spherical geometry will recognize (19) as proportional to the mass flux out of spheres initially saturated with a uniform solute concentration and with a boundary concentration of zero [e.g., *Crank*, 1975, p. 91; *Grathwohl et al.*, 1994].

The resulting late-time approximation for concentration in the mobile domain (with initial concentration of zero) is given by substituting (19) into (12):

$$c = m_0 t_{ad} \beta_{tot} \left(\frac{D_a}{a^2} \right)^2 \sum_{j=1}^{\infty} 6j^2\pi^2 \exp\left(-j^2\pi^2 \frac{D_a}{a^2} t \right). \quad (20)$$

From this expression we can see that the late-time concentration is exponential; therefore on a double-log plot the late-time slope will approach infinity shortly after the mean residence time in the immobile domain ($t_\alpha = a^2/15D_a$) is reached.

Figure 1 shows the full solution to the advection-dispersion mass transfer (ADMT) equations and the late-time approximation. The ADMT equations were solved using STAMMT-L [*Haggerty and Reeves*, 2000] for $m_0 = 1 \times 10^4$ s kg m^{-3}, $t_{ad} = 1 \times 10^4$ s, $D_a/a^2 = 1 \times 10^{-8}$ s^{-1}, $\beta_{tot} = 1$, and Peclet numbers of both 10 and 1000. STAMMT-L is a code that solves (1) with no assumptions other than steady, uniform velocity. It is capable of handling a range of mass transfer models (e.g., first order, diffusion in various geometries, multiple timescales of diffusion, etc.) Since STAMMT-L employs none of the late-time assumptions used in this paper, it is a good check of the mathematics developed here. All concentrations have been nondimensionalized by the terms in front of the infinite series in (20).

From Figure 1 we make four points. First, the approximation very accurately represents the late-time behavior of the ADMT solution (regardless of the Peclet number) but obviously does not contain the advective-dispersive peak. We can see in Figure 1 that the late-time approximation is valid when $t \gg t_{ad}$ provided that $t_\alpha \gg t_{ad}$.

Second, the late-time behavior demonstrates the well-known 3/2 slope for matrix diffusion [e.g., *Hadermann and Heer*, 1996], which ends when $tD_a/a^2 > 1$. As long as the block size a is large enough (or D_a small enough) that $tD_a/a^2 \ll 1$ over the entire time of a tracer test, then the slope remains 3/2. In such a case it would not be possible to estimate the value of D_a/a^2 from the BTC. The limiting case of "infinite" matrix blocks is given in Table 1 for $c \sim dg/dt \sim t^{-3/2}$. Note that the

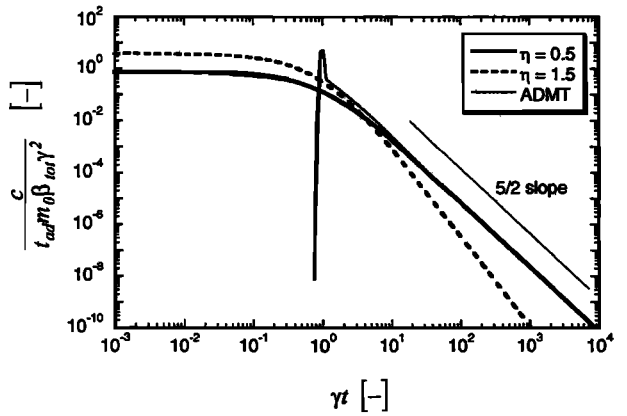

Figure 2. Late-time solution and full ADMT solution for gamma distribution of first-order rate coefficients.

harmonic mean rate coefficient for this case is zero, meaning that the mean residence time for very large blocks approaches infinity.

Third, the location of the BTC peak in the ADMT solution may lie anywhere on the late-time approximation curve, dependent on the relative values of t_{ad} and D_a/a^2.

Last, we note that it is possible to estimate both β_{tot} and D_a/a^2 by using the late-time approximation as a type curve, if the break in slope is present. The capacity coefficient β_{tot} would be estimated from the vertical shift, while D_a/a^2 would be estimated from the horizontal shift.

3.3. Gamma Density Function of First-Order Rate Coefficients

Gamma density functions of rate coefficients have been used to represent multirate mass transfer in several papers. *Cunningham et al.* [1997] developed the mathematics of a gamma density function of diffusion rate coefficients, while *Werth et al.* [1997] applied this model successfully to several mass-fraction-remaining data sets. *Connaughton et al.* [1993] used a gamma density function of first-order rate coefficients to model release of naphthalene from soil, while *Pedit and Miller* [1994] employed a gamma density function of first-order rate coefficients to examine diuron sorption. Other examples include *Ahn et al.* [1996], *Chen and Wagenet* [1997], *Culver et al.* [1997], *Sahoo and Smith* [1997], *Deitsch et al.* [1998], *Kauffman et al.* [1998], *Lorden et al.* [1998], and *Stager and Perram* [1999]. The method we are using is applicable to both types of density functions, and the key relationships for both are given in Table 1. Although the early-time behavior will differ between gamma density functions of first-order and diffusion rate coefficients, the late-time slope will be identical for the same value of η.

The gamma density function of first-order rate coefficients is

$$b(\alpha) = \frac{\beta_{tot}}{\gamma^{\eta}\Gamma(\eta)}\,\alpha^{\eta-1}e^{-\alpha/\gamma}, \tag{21}$$

where γ [T^{-1}] is the scale parameter and η [dimensionless] is the shape parameter. The harmonic mean of (21) is 0 if η is less than 1, a fact that is of particular importance for applications. As a consequence, the mean residence time in the immobile domain would be infinite. (This is also true for gamma density functions of diffusion rate coefficients.) If η is greater than 1, the harmonic mean of (21) is $(\eta - 1)\gamma$.

The memory function is

$$g(t) = -\beta_{tot}\frac{\partial}{\partial t}(\gamma t + 1)^{-\eta}. \tag{22}$$

Therefore the late-time concentration in the mobile domain is given by

$$c = m_0 f_{ad}\beta_{tot}\gamma^2\frac{\eta(\eta+1)}{(\gamma t+1)^{\eta+2}}. \tag{23}$$

Note that when $\gamma t \gg 1$, the BTC follows a power law:

$$c \sim t^{-\eta-2}. \tag{24}$$

The same late-time power law behavior is also exhibited with a density function of diffusion rate coefficients. Note that a power law BTC ($c \sim t^{-k}$) with $k < 3$ would indicate an infinite second (and higher) temporal moment and an infinite mean residence time in the immobile domain.

Figure 2 shows the late-time approximation in (23) nondimensionalized by the transport terms. We have normalized time by the mass transfer rate γ. Figure 2 also shows a solution to the ADMT equations with STAMMT-L [*Haggerty and Reeves*, 2000] for $m_0 = 1 \times 10^4$ s kg m^{-3}, $t_{ad} = 1 \times 10^4$ s, $\gamma = 1 \times 10^{-4}$ s^{-1}, $\eta = 0.5$, $\beta_{tot} = 1$, and a Peclet number of 1000.

We see from (24) and Figure 2 that the late-time double-log slope of concentration will be $-(\eta + 2)$. For comparison to published values, *Connaughton et al.* [1993] estimated values of η in the range of 0.17 to 0.37 for a gamma density function of first-order rate coefficients, while *Pedit and Miller* [1994] estimated $\eta = 0.11$ from their experiments; *Culver et al.* [1997] estimated $\eta = 0.023$ to 0.054 for their column experiments; *Deitsch et al.* [1998] estimated η from 0.092 to 350 in 15 experiments with different materials, with the majority having η below 1. *Kauffman et al.* [1998] estimated $\eta = 0.60$ and 0.84 in two column experiments. *Werth et al.* [1997] found values of η equal to approximately 0.5 for a gamma density function of diffusion rate coefficients. Note that almost all of these estimated η (i.e., those below 1) will lead to an infinite mean residence time within the immobile domain. Consequently, the variance of the breakthrough times will be infinite with these models. Late-time behavior associated with gamma density functions is discussed further in section 4.2.

3.4. Lognormal Density Function of Diffusion Rate Coefficients

Lognormal density functions of rate coefficients have also been used to represent mass transfer in natural systems. *Pedit and Miller* [1994], *Backes et al.* [1995], *Haggerty* [1995], *Culver et al.* [1997], and *McLaren et al.* [1998] all used a lognormal density function of first-order rate coefficients to model uptake and release of sorbing solutes in soils. *Pedit and Miller* [1995] and *Haggerty and Gorelick* [1998] used a lognormal density function of diffusion rate coefficients to model diffusion of sorbing solutes in soils. As is true for the gamma density functions of rate coefficients, the behavior of both lognormal models is very similar, especially at late time and large variances. In our analysis here we will employ only a density function of diffusion rate coefficients:

$$b^*\left(\frac{D_a}{a^2}\right) = \frac{\beta_{tot}}{\sqrt{2\pi}\,\sigma\,\frac{D_a}{a^2}}\exp\left\{-\frac{\left[\ln\left(\frac{D_a}{a^2}\right)-\mu\right]^2}{2\sigma^2}\right\}, \tag{25}$$

where μ and σ are the mean and standard deviation of $\ln (D_a/a^2)$, respectively, in a lognormal distribution. The equivalent density function of first-order rate coefficients is given by *Haggerty and Gorelick* [1998]:

$$b(\alpha) = \sum_{j=1}^{\infty} \frac{8\beta_{tot}}{\sqrt{2\pi^5}\,(2j-1)^2\sigma\alpha} \cdot \exp\left\{ -\frac{\left[\ln\left(\frac{4\alpha}{(2j-1)^2\pi^2}\right) - \mu\right]^2}{2\sigma^2} \right\}. \quad (26)$$

The harmonic mean of (26) is 3 exp $(\mu - \sigma^2/2)$. Consequently, the effective rate coefficient is approximately $0.22\sigma^2$ orders of magnitude smaller than the geometric mean. For large σ the effective rate coefficient is approximately zero, and the mean residence time in the immobile domain approaches infinity. In the limit of very large σ the density function is log-uniform and is equivalent to a power law density function with $\sim\alpha^{-1}$. As we shall see in section 3.5, this corresponds to a late-time BTC of $\sim t^{-2}$.

The Laplace transform of (26) must be done numerically. The result may then be inserted into (12). After taking the second derivative in time (numerically), the late-time approximation for a concentration BTC is shown in Figure 3 for various values of σ. The time axis of Figure 3 is normalized by the geometric mean of (21), and concentration is normalized the same as previously. Figure 3 also shows the solution to the ADMT equations in the presence of a lognormal density function of diffusion rate coefficients. The ADMT equations were solved using STAMMT-L [*Haggerty and Reeves*, 2000] for $m_0 = 1 \times 10^4$ s kg m^{-3}, $t_{ad} = 1 \times 10^4$ s, $e^{\mu} = 1 \times 10^{-4}$ s^{-1}, $\sigma = 5$, $\beta_{tot} = 1$, and a Peclet number of 1000. Note that the late-time slopes for the lognormal distribution lie between 2 and 3 for a large range of time, provided that σ is greater than approximately 3.

Published values of σ for lognormal distributions of rate coefficients are typically larger than 3 [e.g., *Pedit and Miller*, 1994, 1995; *Culver et al.*, 1997; *Haggerty and Gorelick*, 1998; *Haggerty et al.*, 2001], suggesting that mass transfer rate coefficients have large variability in natural media. With such large values of σ we would expect to see late-time slopes on double-log BTCs after a pulse injection between 2 and 3.

3.5. Power Law Density Function of First-Order Rate Coefficients

An alternative density function that has been less commonly used to describe mass transfer in groundwater and soils is a power law density function. *Hatano and Hatano* [1998] used a power law density function of waiting times in the context of a continuous-time random walk to model the sorption of radionuclides in a column experiment. Power law density functions of waiting times have frequently been used in statistical physics to describe anomalous transport behavior [e.g., *Bouchard and Georges*, 1990; *Scher et al.*, 1991]. Frequently, such density functions arise from diffusion or rate-limited sorption on a fractal geometry. A particular advantage of a power law distribution, within the context of this work, is that it allows us to investigate power law BTC behavior for a larger range of late-time slopes.

As with a gamma density function, it is possible to define both a density function of first-order rate coefficients and an equivalent density function of diffusion rate coefficients. Again, although the early time behavior will differ for power law density functions of first-order and diffusion rate coefficients, the late-time slope will be identical for the same value of k. For the sake of brevity, we show only the power law density function of first-order rate coefficients.

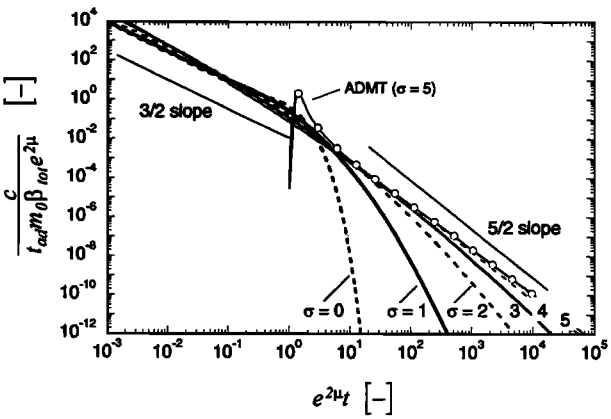

Figure 3. Late-time solution and full ADMT solution for lognormal distribution of diffusion rate coefficients. The value e^{μ} is the geometric mean of the distribution and has units of $[T^{-1}]$.

A truncated power law density function may be written as follows:

$$b(\alpha) = \frac{\beta_{tot}(k-2)}{\alpha_{max}^{k-2} - \alpha_{min}^{k-2}}\,\alpha^{k-3}, \qquad k > 0 \qquad k \neq 2, \quad (27a)$$

$$\alpha_{min} \leq \alpha \leq \alpha_{max},$$

where α_{max} $[T^{-1}]$ is the maximum rate coefficient, α_{min} $[T^{-1}]$ is the minimum rate coefficient, and k is the exponent. The value of α_{min} may be zero if $k > 2$. The reason for choosing to write the power law as $k - 3$ will become apparent shortly. If $k = 2$, the density function may be written

$$b(\alpha) = \frac{\beta_{tot}}{\ln\left(\frac{\alpha_{max}}{\alpha_{min}}\right)}\,\alpha^{-1}. \quad (27b)$$

The late-time concentration in the mobile domain is

$$c = \frac{m_0 t_{ad}\beta_{tot}(k-2)}{(\alpha_{max}^{k-2} - \alpha_{min}^{k-2})} \int_{\alpha_{min}}^{\alpha_{max}} \alpha^{k-1} e^{-\alpha t}\, d\alpha, \qquad k > 0 \qquad k \neq 2. \quad (28)$$

For arbitrary (noninteger) values of k, (28) must, in general, be evaluated numerically. However, the most important point about (28) is that

$$c \sim t^{-k}, \qquad \alpha_{max}^{-1} \ll t \ll \alpha_{min}^{-1}. \quad (29)$$

Expressed in words, the slope of the BTC is k for times much greater than α_{max}^{-1} and much less than α_{min}^{-1} for all values of k. At times greater than α_{min}^{-1}, the slope goes to infinity.

It is possible to present closed-form solutions for many specific cases of (28); we will provide the solutions for the cases $k = 1$, $k = 2$, and $k = 3$. First, let us define three other variables in terms of α_{max} and α_{min}:

$$\tau = \alpha_{max} t, \quad (30a)$$

Table 2. Approximations for the Harmonic Mean of a Truncated Power Law

Approximation to Harmonic Mean $\hat{\alpha}_H$ $[T^{-1}]$	Conditions
$\left(\frac{k-3}{k-2}\right)\alpha_{\min}$	$k < 2$
$\ln(\lambda_t)\alpha_{\min}$	$k = 2$
$-\lambda_t^{k-2}\left(\frac{k-3}{k-2}\right)\alpha_{\min}$	$2 < k < 3$
$\frac{\alpha_{\max}}{\ln(\lambda_t)}$	$k = 3$
$\left(\frac{k-3}{k-2}\right)\alpha_{\max}$	$k > 3$

The exact expression is given in equation (34). Note that all approximations are valid only if $\lambda_t \gg 1$ (i.e., if the ratio of $\alpha_{\max}$ is much greater than $\alpha_{\min}$).

$$\lambda_t = \alpha_{\max}/\alpha_{\min}, \tag{30b}$$

$$\alpha_p^2 = \begin{cases} \dfrac{\alpha_{\max}^2}{1-\lambda_t^{2-k}}, & k \neq 2 \\ \dfrac{\alpha_{\max}^2}{\ln(\lambda_t)}, & k = 2. \end{cases} \tag{30c}$$

Note that α_p is a function of $\alpha_{\max}$, $\alpha_{\min}$, and k and is used for the purpose of simplifying the following equations only.

Using these variables, the late-time concentration for $k = 1$ is therefore

$$c = m_0 t_{ad}\beta_{tot}\alpha_p^2(e^{-\tau/\lambda_t} - e^{-\tau})\tau^{-1}. \tag{31}$$

If $k = 2$, then the density function is log-uniform, and the late-time concentration is

$$c = m_0 t_{ad}\beta_{tot}\alpha_p^2\left[e^{-\tau/\lambda_t}\left(\frac{\tau}{\lambda_t}+1\right) - e^{-\tau}(\tau+1)\right]\tau^{-2}. \tag{32}$$

If $k = 3$, then the density function is uniform, and the late-time concentration is

$$c = m_0 t_{ad}\beta_{tot}\alpha_p^2\left[e^{-\tau/\lambda_t}\left(\frac{\tau^2}{\lambda_t^2}+\frac{2\tau}{\lambda_t}+2\right) - e^{-\tau}(\tau^2+2\tau+2)\right]\tau^{-3}. \tag{33}$$

From the above equations we see that a family of curves is required for each value of k since both $\alpha_{\min}$ and $\alpha_{\max}$ appear in all equations. However, inspection of the equations indicates that the curves for each value of k will be identical until t approaches $\alpha_{\min}^{-1}$.

The harmonic mean of the density function (27a) and (27b) is

$$\hat{\alpha}_H = \begin{cases} \ln(\lambda_t)\dfrac{\alpha_{\min}\lambda_t}{\lambda_t - 1}, & k = 2, \\ \dfrac{\alpha_{\max}}{\ln(\lambda_t)}, & k = 3, \\ \alpha_{\min}\dfrac{(k-3)\,\lambda_t^{k-2}-1}{(k-2)\,\lambda_t^{k-3}-1}, & \text{otherwise.} \end{cases} \tag{34}$$

Approximations (see Table 2) may be made to (34) that are useful in understanding what controls the harmonic mean of the distribution. Note again that the mean residence time in the immobile domain is simply the inverse of $\hat{a}_H$.

We make two points in regard to (34) and Table 2 and leave further discussion of late-time behavior associated with power law density functions to section 4.2. First, if the late-time slope of the BTC is less than 3 (i.e., $k < 3$), then the harmonic mean is controlled by $\alpha_{\min}$. The parameter $\alpha_{\min}$ cannot be estimated from a BTC, however, if the late-time behavior of the BTC remains power law until the end of the experiment. Consequently, the harmonic mean (and therefore the mean residence time in the immobile domain) cannot be estimated if the behavior of the BTC remains power law until the end of the experiment, with a slope less than 3.

Second, if $k < 3$ and $\alpha_{\min} = 0$, then the harmonic mean is 0. Therefore, if a BTC has a late-time slope of $k < 3$ and the behavior is due to mass transfer, this may indicate an infinite mean residence time in the immobile domain. It also causes the second and higher temporal moments of the BTC to be infinite.

Note that there is nothing that physically precludes a late-time slope between 2 and 3 being maintained to infinite time (i.e., $2 < k < 3$ as $t \to \infty$). A slope of $k \leq 2$ to infinite time, however, would require an infinitely large immobile domain (i.e., infinite capacity). Therefore a slope of $k \leq 2$ cannot be maintained for infinite time (for this reason, $k = 3/2$ is possible with diffusion but only until a time of $\sim a^2/D_a$).

The late-time behavior of concentration, as given by (31)–(33), is shown in Figure 4 for $\alpha_{\min} = 10^{-5}\,\alpha_{\max}$. Figure 4 also shows the solution to the ADMT equations in the presence of a power law density function of rate coefficients. The ADMT equations were solved using STAMMT-L [*Haggerty and Reeves*, 2000] for $m_0 = 1$ s kg m^{-3}, $t_{ad} = 1$ s, $\alpha_{\max} = 1$ s^{-1}, $\alpha_{\min} = 1 \times 10^{-5}$ s^{-1}, $k = 1$, $\beta_{tot} = 1$, and a Peclet number of 1000.

3.6. Summary of Late-Time Slopes

Figure 5 provides a summary of late-time slopes for several of the models presented. Late-time slopes are given versus nondimensional time. Note that a BTC with advection and dispersion will mask some portion of the slopes shown in Figure 5 at earlier times. The slopes given in Figure 5 will only be present when $t \gg t_{ad}$. A power law slope is a constant at late time, such as provided by the gamma and power law density functions. Note that conventional diffusion model is equivalent to the lognormal density function with $\sigma = 0$. The slope in the conventional model is 3/2 until approximately the mean residence time in the immobile domain ($a^2/3D_a$ for one-

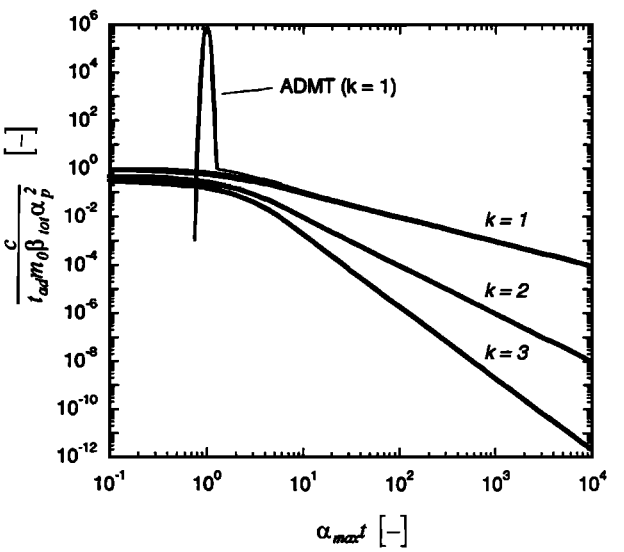

Figure 4. Late-time solution and full ADMT solution for power law distribution of first-order rate coefficients.

dimensional diffusion). Note that the lognormal density function with larger σ cannot provide a true power law BTC but can hold the slope relatively constant over a long time. All lognormal density functions will approach an infinite slope as time goes to infinity.

4. Applications to Tracer Tests and Discussion

4.1. WIPP Tracer Tests

Figure 6a shows data and confidence intervals from two single-well injection-withdrawal (SWIW) tracer tests conducted in the Culebra Dolomite Member of the Rustler Formation at the Waste Isolation Pilot Plant (WIPP) site in southeastern New Mexico. The Culebra is a 7-m-thick, variably fractured dolomite and is a potential pathway to the accessible environment in the event of a radionuclide release from the WIPP. These two tests were performed in the central well at two multiwell sites, designated H11 and H19. The SWIW tests consisted of the consecutive injection of one or more slugs of conservative tracers into the Culebra Dolomite, followed by the injection of a Culebra brine chaser (containing no tracer), and then followed by a resting period of approximately 6.5×10^4 s (18 hours). The tracers were then removed from the formation by pumping on the same well until concentration was close to or below detection levels. The total residence time (i.e., t_{ad}) of the slug in the formation was approximately 9.0×10^4 s (25 hours). Details of the tracer tests are given by *Meigs and Beauheim* [2001] and by *Meigs et al.* [2000]. Interpretation of the SWIW tests by *Haggerty et al.* [2001] suggests that the late-time behavior of the BTC is due to multiple rates of mass transfer. It is clear that neither heterogeneity nor tracer drift alone can be responsible for the observed behavior, though a combination of the two may explain some fraction of it [*Lessoff and Konikow*, 1997; *Meigs et al.*, 2000; *Haggerty et al.*, 2001].

Note that although the SWIW tests have a velocity field that changes in both space and time, our method is still applicable. First, the method is not limited to spatially uniform velocity fields (provided that residence time distribution in the immobile domain is spatially uniform, although this restriction will be relaxed in a future paper), so the radial nature of the velocity field is not a limitation. Second, the transient nature of the velocity field is of minor importance, because the transience is at very early time (prior to 9.0×10^4 s or 25 hours). Since the transience is of very small time relative to the timescales of mass transfer that we are interested in, the transience does not influence the analysis.

The SWIW data in Figure 6a display late-time slopes that are approximately constant over several hundred hours. The slopes at all times for both BTCs are given in Figure 6b, which was calculated using a five-point, moving-window average. As

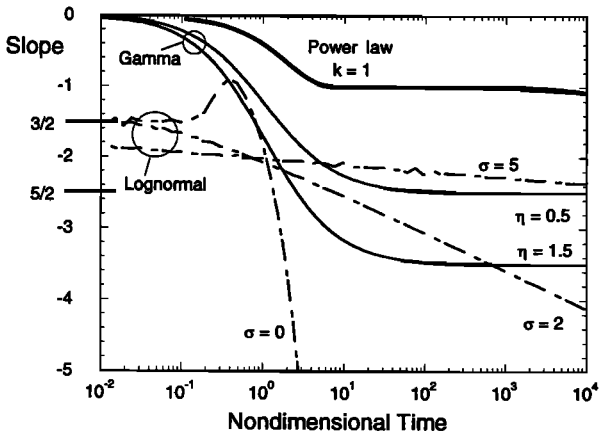

Figure 5. Slopes of late-time double-log breakthrough curves (BTC). Note that during the time that the BTC is dominated by advection and dispersion (i.e., at early time), the slopes will be different from those shown here. Nondimensional time is given as in Figures 1, 2, 3, and 4 for each of the models.

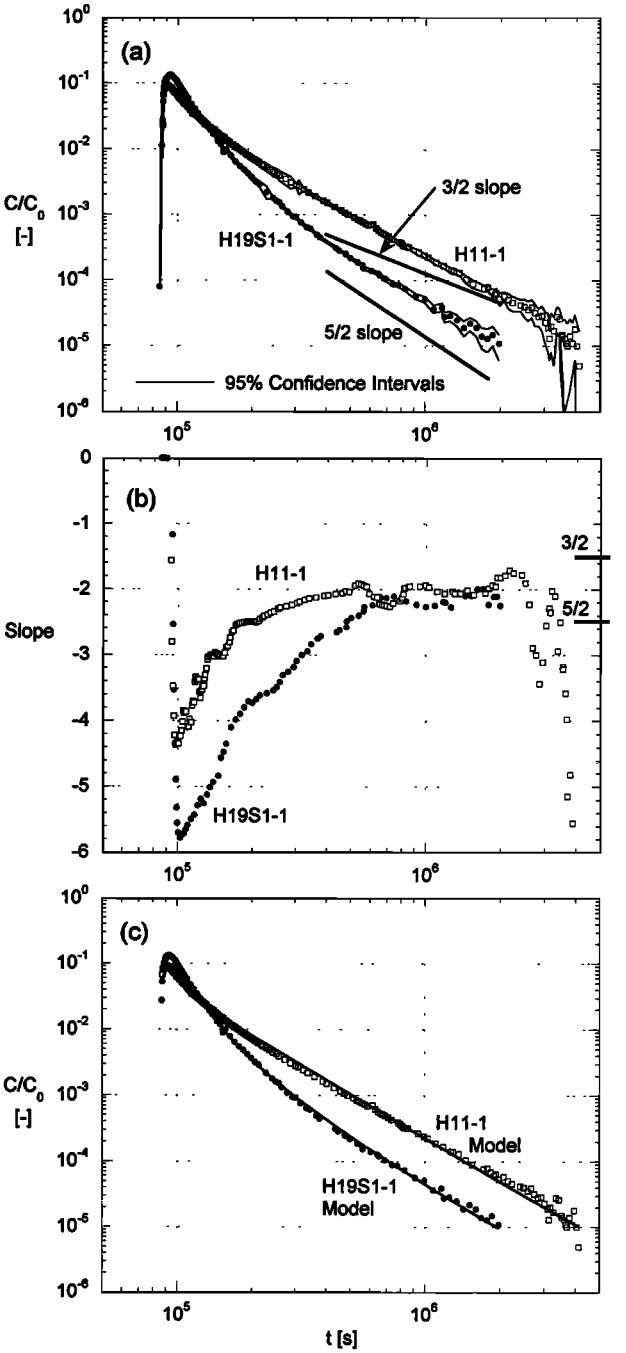

Figure 6. Plots of single-well injection-withdrawal data from (a) the Waste Isolation Pilot Plant site, (b) the slopes of the data, and (c) an advection-dispersion mass transfer model of the data.

can be seen from Figures 6a and 6b, the late-time behavior of both BTCs is essentially power law. The H11-1 BTC has a slope of about 2.123 after 2.5×10^5 s (69 hours). The slope of the H11-1 BTC appears to become more negative after about 3×10^6 s (830 hours), but this may be due to a 70% increase in the pumping rate at that time. In addition, the accuracy of the data is relatively low after 2×10^6 s, making slope calculations uncertain. The H19S1-1 BTC has a constant slope of about 2.165 from 5×10^5 s (139 hours) to the end of the test. Note that conventional (single rate) diffusion can only provide a constant late-time slope of 3/2, which is shown for comparison in Figure 6a.

The late-time behavior of the SWIW tests was interpreted by *Haggerty et al.* [2001] using a lognormal density function of diffusion rate coefficients (D_a/a^2). As shown in that paper, a lognormal density function does an excellent job of representing the entire BTC (with $\sigma = 3.55$ for H11-1 and $\sigma = 6.87$ for H19S1-1). However, on the basis of the BTC data alone it is not possible to rule out other density functions of rate coefficients, including a gamma density function or a power law density function.

4.2. Implications Power Law BTC Behavior

We note again that both the gamma and power law density functions result in power law BTCs at late time, with the relationship $k = \eta + 2$. The conventional diffusion model also causes power law BTCs with a slope of 3/2 prior to $t \sim a^2/D_a$. There are four important scenarios for such power law behavior.

4.2.1. Case 1: Power law behavior to infinite time and $k \leq 3$. The first scenario is that the BTC behaves as a power law over all time (i.e., the slope of the BTC would be power law to infinite time) and that the slope is less than 3. It is important to note that (1) this is physically possible provided that the slope k is also greater than 2 and (2) several papers effectively invoke case 1 by assuming a gamma density function and finding estimates of η less than 1 [e.g., *Connaughton et al.*, 1993; *Pedit and Miller*, 1994; *Culver et al.*, 1997; *Werth et al.*, 1997; *Deitsch et al.*, 1998; *Kauffman et al.*, 1998; *Lorden et al.*, 1998]. In case 1 the mean residence time in the immobile domain must be infinite. Consequently, there can be no effective single-rate model that is equivalent to the multirate model in the way that a single-rate first-order model is approximately equivalent to a conventional single-rate diffusion model. No single-rate (either first order or diffusion) model can yield the same second or higher temporal moments as the multirate model. In fact, any single-rate model (either first order or diffusion) fit to data will have parameters that are a function of the experimental observation time (i.e., the experiment length).

4.2.2. Case 2: Power law behavior longer than experimental timescale and $k \leq 3$. The second scenario is that the power law behavior ends at a particular time that is beyond the experimental observation time and that the slope is less than 3. In this case the mean residence time in the immobile domain cannot be ascertained from the experimental data alone. In other words, it is impossible, based solely on the BTC data, to estimate an effective rate coefficient: The effective rate coefficient could be either undefined (as in case 1) or simply longer than the inverse of the experimental time.

If the slope k is less than 2, then the power law behavior either must end at some time or the slope must steepen to greater than 2. Such is the case with conventional diffusion and a slope of 3/2. Because the immobile domain cannot be infinitely thick, the power law behavior with k less than 2 must end at some time. However, without information external to the tracer test data the time at which the power law behavior ends (and therefore the mean residence time in the immobile domain) cannot be known.

4.2.3. Case 3: Power law behavior ends within experimental timescale. The third scenario is that the power law behavior ends within the experimental observation time. An example of this is the conventional diffusion model with a slope of 3/2 at intermediate time. In this case an effective rate coefficient or mean residence time in the immobile domain can be estimated. The mean residence time will be larger for smaller slopes and for very small slopes will approach the inverse of the time at which the power law behavior ends. Note that case 3 cannot be modeled by a gamma density function because a gamma density function does not allow for an end to the power law behavior.

4.2.4. Case 4: Power law behavior with $k > 3$. The fourth scenario is that the BTC has a slope greater than 3. In this case the mean residence time can be estimated even if the power law behavior extends to infinite time. This is because the harmonic mean of a power law density function is nonzero and dominated by the value of α_{max}, provided that $k > 3$.

Which scenario do the WIPP SWIW tracer tests fit? On the basis of the BTC data alone, H19S1-1 must be either case 1 or case 2. Since the power law behavior extends to the end of the data set, it is not possible to estimate the mean residence time of the immobile domain. We know only that the mean residence time must be at least the inverse of the experimental time (i.e., $\sim 1.9 \times 10^6$ s). H11-1, however, may be case 3. If the marked change in slope at approximately 3×10^6 s is not primarily due to the increase in pumping rate, then H11-1 is case 3. However, if this is an artifact of the increase in pumping rate, then H11-1 may be case 1 or 2. Given the data uncertainty after approximately 2×10^6 s (560 hours) and the fact that we have not investigated the case of time-varying pumping rate, we remain uncertain as to which case H11-1 fits.

Models of the two breakthrough curves were constructed and are shown in Figure 6c. In both cases a gamma distribution of rate coefficients was used to model mass transfer, which yields a power law BTC with late-time behavior of $t^{-\eta-2}$ (i.e., slope of $k = \eta + 2$). In addition to mass transfer the model simulated advection and dispersion radially away from a well, a brief resting period, and advective-dispersive transport back to the well (more details on the transport code are given by *Haggerty et al.* [2000, 2001]). Since H11-1 exhibits an average late-time slope of 2.123 (measured directly from the data), we modeled it with $\eta = 0.123$. The only estimated parameters in this model were γ (3.05×10^{-5} s^{-1}), the advective porosity (0.0158), and the dispersivity (0.151 m). Since H19S1-1 exhibits an average late-time slope of about 2.165, we modeled it with $\eta = 0.165$. Again, the only estimated parameters in this model were γ (2.96×10^{-4} s^{-1}), the advective porosity (0.0679), and the dispersivity (0.115 m). In both models all other parameters were taken from field measurements and the model of *Haggerty et al.* [2001, Tables 1 and 3]. In both H11-1 and H19S1-1 the late-time behavior of the data could have been modeled with only a single estimated parameter, advective porosity. However, the other parameters were estimated to fit the peak of the BTC.

It can be seen that both models are very good representations of the SWIW data, particularly at late time. It is worth noting that the parameter η determining the late-time slope of

the BTCs was simply read from the data and not fit. This good representation of the late-time data emphasizes three points: (1) The late-time approximation is a good tool for analyzing BTCs; (2) the approximation does not depend on uniform velocity; and (3) the approximation does not depend on a Dirac injection pulse or negligible dispersion to work well.

5. Conclusions

With improvements in experimental and analytical techniques, breakthrough curves (BTCs) are now available from many laboratory and field experiments with several orders of magnitude of data in both time and concentration. The late-time behavior of BTCs is critically important for the evaluation of rate-limited mass transfer, especially if discrimination between different models of mass transfer is desired. Double-log plots of BTCs are particularly helpful and commonly yield valuable information about mass transfer.

We have seven primary conclusions. First, we derived a simple analytical expression for late-time BTC behavior in the presence of mass transfer. Equation (12) gives the late-time concentration for any linear rate-limited mass transfer model for either zero-concentration or equilibrium initial conditions. The expression requires the advection timescale, the zeroth moment of the injection pulse, the initial concentration in the system, and the memory function $g(t)$ be known. Note that caution is advised in using (12) if the variance of t_{ad} is large (such as in a strongly heterogeneous velocity field). We expect that (12) will be exploited to understand breakthrough curves from field and laboratory experiments, as well as to develop criteria for designing better tracer tests to meet specific goals (e.g., estimating mass transfer rate coefficients).

Second, the memory function $g(t)$ is proportional to the residence time distribution in the immobile domain given a unit impulse at the surface of the immobile domain. This memory function is simply the derivative of the Laplace transform of the density function of rate coefficients describing the immobile domain. Consequently, the late-time concentration is proportional to the first or second derivative of the Laplace transform of the density function of rate coefficients.

Third, the effective rate coefficient that yields the same zeroth, first, and second BTC temporal moments as does the full density function is the harmonic mean of the density function of rate coefficients. However, for any density function of rate coefficients with power law α^{k-3} as $\alpha \rightarrow 0$ and where $k \leq 3$, the harmonic mean is zero. Consequently, the mean residence time in the immobile domain is infinite, and there is no single effective rate coefficient. This applies both to density functions of diffusion rate coefficients and density functions of first-order rate coefficients. Many such distributions have been invoked in the literature.

Fourth, if the BTC (after a pulse injection) goes as $\sim t^{-k}$ as $t \rightarrow \infty$, then the underlying density function of rate coefficients must be $\sim \alpha^{k-3}$ as $\alpha \rightarrow 0$. This holds for density functions of both first-order and diffusion rate coefficients. For a BTC from a medium with initially nonzero but equilibrium concentrations, the equivalent BTC goes as t^{1-k}.

Fifth, if the slope of a BTC (after a pulse injection) goes to k as $t \rightarrow \infty$ and $k \leq 3$, then the mean residence time in the immobile domain is infinite. (This is a corollary to the third and fourth conclusions.) Consequently, there is no single effective rate coefficient in this medium. A second consequence is that any single-rate (either diffusion or first order) rate coefficient estimated from the BTC will be a function of experimental observation time. Again, for a BTC from a medium with initially nonzero but equilibrium concentrations, the equivalent BTC goes as t^{-k+1}.

Sixth, if a BTC exhibits power law behavior ($c \sim t^{-k}$) to the end of the experiment, then one of two cases must exist. If $k \leq 3$, then the mean residence time (and effective rate coefficient) cannot be estimated from the BTC. The mean residence time must be at least the experimental observation time and could be infinite. If $k > 3$, then the mean residence time (and its inverse, the effective rate coefficient) can be estimated.

Seventh, the late-time approximation does not strictly depend on several of the assumptions used in its derivation. The approximation was able to adequately characterize a distribution of mass transfer rate coefficients from a single-well injection-withdrawal tracer test, which has conditions of radial time-varying flow, significant dispersion, and a nonpulse-type injection.

Appendix A: Notes on the Density Function $b(\alpha)$

We add two notes regarding the density function $b(\alpha)$. First, a useful definition is that of the zeroth moment of the density function of rate coefficients:

$$\int_0^\infty b(\alpha)\, d\alpha = \beta_{tot}, \tag{A1}$$

where β_{tot} [dimensionless] is commonly known as the capacity coefficient [e.g., *Haggerty and Gorelick*, 1995]. The capacity coefficient is the ratio of mass in the immobile domain to mass in the mobile domain at equilibrium; in the absence of sorption it is the ratio of the two volumes.

Second, we note without derivation that the Laplace transform of the density function of rate coefficients is a particularly useful function by itself. This function is proportional to the mass fraction remaining in the immobile domain, where the initial conditions are uniform concentration in the immobile domain and the boundary condition on the immobile domain is zero concentration. The mass fraction (M/M_0) remaining in the medium (both mobile and immobile domains) at late time is therefore

$$\frac{M(t)}{M_0} = \frac{\mathcal{L}\{b(\alpha)\}}{1+\beta_{tot}} = \frac{\int_0^\infty b(\alpha) e^{-\alpha t}\, d\alpha}{1+\beta_{tot}}, \tag{A2}$$

where $M(t)$ is the mass at any time and M_0 is the total initial mass. In other words, the mass fraction remaining within, for example, a column after several pore volumes have been flushed through it, is calculated simply by finding the Laplace transform of the density function $b(\alpha)$.

Appendix B: Notes on Application of Equation (12)

Equation (12) presents an interesting theoretical development for two reasons. First, the late-time behavior of the BTC is easily obtained for a wide variety of density functions $b(\alpha)$ using any comprehensive table of Laplace transforms. Equation (12) is simpler for first-order mass transfer than the equations developed by *Vereecken et al.* [1999]. The equation also

provides an asymptotic expression for any mass transfer process with a known memory function $g(t)$, which is easily calculated for a wide range of sorption and diffusion processes. Conversely, it must be pointed out that the equations developed by *Vereecken et al.* [1999] allow for time-varying velocity.

Second, (12) suggests that the density function of mass transfer rate coefficients (whether from diffusion, nonequilibrium sorption, or a general density function of mass transfer processes) is available directly and analytically from breakthrough data. In fact, if (12) is treated as an integral equation where $b(\alpha)$ is an unknown, the density function $b(\alpha)$ may be directly calculated using the inverse Laplace transform. If the medium is initially free of tracer, then $c_0 = 0$ and the density function $b(\alpha)$ is given analytically by the Bromwich integral:

$$b(\alpha) = \frac{1}{t_{ad} m_0 \alpha^2 (2\pi i)} \int_{Br} c(x = L, t) e^{\alpha t}\, dt$$

$$= \frac{1}{t_{ad} m_0 \alpha^2} \mathcal{L}^{-1}\{c(x = L, t)\}, \qquad \text{(B1)}$$

where i is the unit imaginary number and Br represents the Bromwich contour [see, e.g., *LePage*, 1961, pp. 319–320]. A similar equation may be easily constructed for the case of nonzero initial conditions and continuous flushing of tracer-free fluid, such as in a purge experiment. Unfortunately, the practical use of (B1) is limited by the conditions that we can only use the late-time breakthrough data and that scatter in the data introduce numerical instabilities in the inverse Laplace transform. Nonetheless, (B1) will allow us to determine certain important properties of the density function $b(\alpha)$.

For relatively simple cases (i.e., single-rate mass transfer) the properties of (12) allow estimation of the rate coefficient and capacity coefficient directly from the BTC [also see *Vereecken et al.*, 1999]. For some more complex cases (e.g., gamma and power law density functions) the properties of (12) allow certain properties of the density function of rate coefficients to be determined.

Acknowledgments. This work was funded by Sandia National Laboratories and by the Swedish Nuclear Fuel and Waste Management Co. (SKB). Sandia is a multiprogram laboratory operated by Sandia Corporation, a Lockheed Martin Company, for the United States Department of Energy under contract DE-AC04-94AL85000. R.H. would like to thank A. T. Zoes for helpful conversations in regard to this work. We are grateful for reviews by B. Berkowitz, J. Cunningham, V. Cvetkovic, B. Davis, S. Geiger, P. Reeves, and three anonymous reviewers and for logistical support provided by M. Kelley.

References

Ahn, I. S., L. W. Lion, and M. L. Shuler, Microscale-based modeling of polynuclear aromatic hydrocarbon transport and biodegradation in soil, *Biotechnol. Bioeng.*, *51*(1), 1–14, 1996.

Albery, W. J., P. N. Bartlett, C. P. Wilde, and J. R. Darwent, A general model for dispersed kinetics in heterogeneous systems, *J. Am. Chem. Soc.*, *107*(7), 1854–1858, 1985.

Backes, E. A., R. G. McLaren, A. W. Rate, and R. S. Swift, Kinetics of cadmium and cobalt desorption from iron and manganese oxides, *Soil Sci. Soc. Am. J.*, *59*(3), 778–785, 1995.

Berkowitz, B., and H. Scher, Anomalous transport in random fracture networks, *Phys. Rev. Lett.*, *79*(20), 4038–4041, 1997.

Bouchaud, J.-P., and A. Georges, Anomalous diffusion in disordered media: Statistical mechanisms, models and physical applications, *Phys. Rep.*, *195*(4–5), 127–293, 1990.

Brusseau, M. L., R. E. Jessup, and P. S. C. Rao, Modeling the transport of solutes influenced by multiprocess nonequilibrium, *Water Resour. Res.*, *25*(9), 1971–1988, 1989.

Cameron, D. R., and A. Klute, Convective-dispersive solute transport with a combined equilibrium and kinetic adsorption model, *Water Resour. Res.*, *13*(1), 183–188, 1977.

Carrera, J., X. Sánchez-Vila, I. Benet, A. Medina, G. Galarza, and J. Guimerà, On matrix diffusion: Formulations, solution methods and qualitative effects, *Hydrogeol. J.*, *6*(1), 178–190, 1998.

Chen, W., and R. J. Wagenet, Solute transport in porous media with sorption-site heterogeneity, *Environ. Sci. Technol.*, *29*(11), 2725–2734, 1995.

Chen, W., and R. J. Wagenet, Description of atrazine transport in soil with heterogeneous nonequilibrium sorption, *Soil Sci. Soc. Am. J.*, *61*(2), 360–371, 1997.

Coats, K. H., and B. D. Smith, Dead-end pore volume and dispersion in porous media, *Soc. Pet. Eng. J.*, *4*(1), 73–84, 1964.

Connaughton, D. F., J. R. Stedinger, L. W. Lion, and M. L. Shuler, Description of time-varying desorption kinetics: Release of naphthalene from contaminated soils, *Environ. Sci. Technol.*, *27*(12), 2397–2403, 1993.

Crank, J., *The Mathematics of Diffusion*, 2nd ed., Oxford Univ. Press, New York, 1975.

Culver, T. B., S. P. Hallisey, D. Sahoo, J. J. Deitsch, and J. A. Smith, Modeling the desorption of organic contaminants from long-term contaminated soil using distributed mass transfer rates, *Environ. Sci. Technol.*, *31*(6), 1581–1588, 1997.

Cunningham, J. A., and P. V. Roberts, Use of temporal moments to investigate the effects of nonuniform grain-size distribution on the transport of sorbing solutes, *Water Resour. Res.*, *34*(6), 1415–1425, 1998.

Cunningham, J. A., C. J. Werth, M. Reinhard, and P. V. Roberts, Effects of grain-scale mass transfer on the transport of volatile organics through sediments, 1, Model development, *Water Resour. Res.*, *33*(12), 2713–2726, 1997.

Deitsch, J. J., J. A. Smith, M. B. Arnold, and J. Bolus, Sorption and desorption rates of carbon tetrachloride and 1,2-dichlorobenzene to three organobentonites and a natural peat soil, *Environ. Sci. Technol.*, *32*(20), 3169–3177, 1998.

Eikenberg, J., E. Hoehn, T. Fierz, and U. Frick, Grimsel Test Site: Preparation and performance of migration experiments with radioisotopes of sodium, strontium and iodine, *PSI-Ber. 94-11*, Paul Scherrer Inst., Würenlingen, Switzerland, 1994.

Farrell, J., and M. Reinhard, Desorption of halogenated organics from model solids, sediments, and soil under unsaturated conditions, 2, Kinetics, *Environ. Sci. Technol.*, *28*(1), 63–72, 1994.

Fong, F. K., and L. A. Mulkey, Solute transport in aggregated media: Aggregated size distribution and mean radii, *Water Resour. Res.*, *26*(6), 1291–1303, 1990.

Glueckauf, E., Theory of chromatography, 10, Formulae for diffusion into spheres and their application to chromatography, *Trans. Faraday Soc.*, *51*(11), 1540–1551, 1955.

Grathwohl, P., W. Pyka, and P. Merkel, Desorption of organic pollutants (PAHs) from contaminated aquifer material, in *Transport and Reactive Processes in Aquifers*, edited by T. Dracos and F. Stauffer, pp. 469–474, A. A. Balkema, Brookfield, Vt., 1994.

Hadermann, J., and W. Heer, The Grimsel (Switzerland) migration experiment: Integrating field experiments, laboratory investigations and modelling, *J. Contam. Hydrol.*, *21*(1–4), 87–100, 1996.

Haggerty, R., Aquifer remediation in the presence of rate-limited mass transfer, Ph.D. dissertation, Stanford Univ., Stanford, Calif., 1995.

Haggerty, R., and S. M. Gorelick, Multiple-rate mass transfer for modeling diffusion and surface reactions in media with pore-scale heterogeneity, *Water Resour. Res.*, *31*(10), 2383–2400, 1995.

Haggerty, R., and S. M. Gorelick, Modeling mass transfer processes in soil columns with pore-scale heterogeneity, *Soil Sci. Soc. Am. J.*, *62*(1), 62–74, 1998.

Haggerty, R., and P. Reeves, *STAMMT-L: Solute Transport and Multirate Mass Transfer*, User's manual, Sandia Natl. Lab., Albuquerque, N. M., in press, 2000.

Haggerty, R., S. W. Fleming, and S. A. McKenna, STAMMT-R: Solute transport and multirate mass transfer in radial coordinates, Version 1.01, *Rep. SAND99-0164*, Sandia Natl. Lab., Albuquerque, N. M., 2000.

Haggerty, R., S. W. Fleming, L. C. Meigs, and S. A. McKenna, Tracer tests in a fractured dolomite, 2, Analysis of mass transfer in single-well injection-withdrawal tests, *Water Resour. Res.*, in press, 2001.

Hatano, Y., and N. Hatano, Dispersive transport of ions in column experiments: An explanation of long-tailed profiles, *Water Resour. Res.*, *34*(5), 1027–1033, 1998.

Hollenbeck, K. J., C. F. Harvey, R. Haggerty, and C. J. Werth, A method for estimating distributions of mass transfer rate coefficients with application to purging and batch experiments, *J. Contam. Hydrol.*, *37*(3–4), 367–388, 1999.

Jaekel, U., A. Georgescu, and H. Vereecken, Asymptotic analysis of nonlinear equilibrium solute transport in porous media, *Water Resour. Res.*, *32*(10), 3093–3098, 1996.

Kauffman, S. J., C. H. Bolster, G. M. Hornberger, J. S. Herman, and A. L. Mills, Rate-limited transport of hydroxyatrazine in an unsaturated soil, *Environ. Sci. Technol.*, *32*(20), 3137–3141, 1998.

Lafolie, F., and C. Hayot, One-dimensional solute transport modelling in aggregated porous media, 1, Model description and numerical solution, *J. Hydrol.*, *143*(1–2), 63–83, 1993.

LePage, W. R., *Complex Variables and the Laplace Transform for Engineers*, McGraw-Hill, New York, 1961.

Lessoff, S. C., and L. F. Konikow, Ambiguity in measuring matrix diffusion with single-well injection/recovery tracer tests, *Ground Water*, *35*(1), 166–176, 1997.

Lorden, S. W., W. Chen, and L. W. Lion, Experiments and modeling of the transport of trichloroethene vapor in unsaturated aquifer material, *Environ. Sci. Technol.*, *32*(13), 2009–2017, 1998.

McLaren, R. G., C. A. Backes, A. W. Rate, and R. S. Swift, Cadmium and cobalt desorption-kinetics from soil clays: Effect of sorption period, *Soil Sci. Soc. Am. J.*, *62*(2), 332–337, 1998.

Meigs, L. C., and R. L. Beauheim, Tracer tests in a fractured dolomite, 1, Experimental design and observed tracer recoveries, *Water Resour. Res.*, in press, 2001.

Meigs, L. C., R. L. Beauheim, and T. L. Jones (Eds.), Interpretations of tracer tests performed in the Culebra dolomite at the Waste Isolation Pilot Plant site, *Rep. SAND97-3109*, Sandia Natl. Lab., Albuquerque, N. M., 2000.

Neretnieks, I., and A. Rasmuson, An approach to modeling radionuclide migration in a medium with strongly varying velocity and block sizes along the flow path, *Water Resour. Res.*, *20*(12), 1823–1836, 1984.

Pedit, J. A., and C. T. Miller, Heterogeneous sorption processes in subsurface systems, 1, Model formulations and applications, *Environ. Sci. Technol.*, *28*(12), 2094–2104, 1994.

Pedit, J. A., and C. T. Miller, Heterogeneous sorption processes in subsurface systems, 2, Diffusion modeling approaches, *Environ. Sci. Technol.*, *29*(7), 1766–1772, 1995.

Peszyńska, M., Finite element approximation of diffusion equations with convolution terms, *Math. Comput.*, *65*(215), 1019–1037, 1996.

Rao, P. S. C., D. E. Rolston, R. E. Jessup, and J. M. Davidson, Solute transport in aggregated porous media: Theoretical and experimental evaluation, *Soil Sci. Soc. Am. J.*, *44*(6), 1139–1146, 1980.

Rao, P. S. C., R. E. Jessup, and T. M. Addiscott, Experimental and theoretical aspects of solute diffusion in spherical and nonspherical aggregates, *Soil Sci.*, *133*(6), 342–349, 1982.

Rasmuson, A., The effect of particles of variable size, shape and properties on the dynamics of fixed beds, *Chem. Eng. Sci.*, *40*(4), 621–629, 1985.

Roberts, G. E., and H. Kaufman, *Table of Laplace Transforms*, W. B. Saunders, Philadelphia, Pa., 1966.

Ruthven, D. M., and K. F. Loughlin, The effect of crystallite shape and size distribution on diffusion measurements in molecular sieves, *Chem. Eng. Sci.*, *26*(5), 577–584, 1971.

Sahoo, D., and J. A. Smith, Enhanced trichloroethene desorption from long-term contaminated soil using triton X-100 and pH increases, *Environ. Sci. Technol.*, *31*(7), 1910–1915, 1997.

Scher, H., M. F. Shlesinger, and J. T. Bendler, Time-scale invariance in transport and relaxation, *Phys. Today*, *44*(1), 26–34, 1991.

Stager, M. P., and G. P. Perram, Long-term desorption of trichloroethylene from flint clay using multiplexed optical detection, *Environ. Pollut.*, *104*(3), 397–400, 1999.

Valocchi, A. J., Use of temporal moment analysis to study reactive solute transport in aggregated porous media, *Geoderma*, *46*(1/3), 233–247, 1990.

van Genuchten, M. T., and P. J. Wierenga, Mass transfer studies in sorbing porous media, 1, Analytical solutions, *Soil Sci. Soc. Am. J.*, *40*(4), 473–480, 1976.

Vereecken, H., U. Jaekel, and A. Georgescu, Asymptotic analysis of solute transport with linear nonequilibrium sorption in porous media, *Transp. Porous Media*, *36*(2), 189–210, 1999.

Villermaux, J., Deformation of chromatographic peaks under the influence of mass transfer phenomena, *J. Chromatogr. Sci.*, *12*, 822–831, 1974.

Villermaux, J., Theory of linear chromatography, in *Percolation Processes: Theory and Applications*, *NATO ASI Ser. E*, edited by E. Rodrigues and D. Tondeur, vol. 33, pp. 83–140, Sijthoff and Noordhoff, Rockville, Md., 1981.

Wagner, B. J., and J. W. Harvey, Experimental design for estimating parameters of rate-limited mass transfer: Analysis of stream tracer studies, *Water Resour. Res.*, *33*(7), 1731–1741, 1997.

Werth, C. J., J. A. Cunningham, P. V. Roberts, and M. Reinhard, Effects of grain-scale mass transfer on the transport of volatile organics through sediments, 2, Column results, *Water Resour. Res.*, *33*(12), 2727–2740, 1997.

R. Haggerty, Department of Geosciences, Oregon State University, Corvallis, OR 97331-5506. (haggertr@geo.orst.edu)

S. A. McKenna and L. C. Meigs, Geohydrology Department, Sandia National Laboratories, P.O. Box 5800, MS-0735, Albuquerque, NM 87185-0735. (samcken@nwer.sandia.gov; lcmeigs@nwer.sandia.gov)

(Received October 4, 1999; revised May 4, 2000;
accepted July 17, 2000.)